Open Research Online

Acid Dissociation Equilibrium and Singlet Molecular Oxygen Quantum Yield of Acetylated 6,8–Dithioguanosine in Aqueous Buffer Solution

Journal Item

For guidance on citations see FAQs.

Version: Accepted Manuscript

Link(s) to article on publisher's website:
http://dx.doi.org/doi:10.1021/acs.jpcb.8b00517

oro.open.ac.uk

Acid Dissociation Equilibrium and Singlet Molecular Oxygen Quantum Yield of Acetylated 6,8–Dithioguanosine in Aqueous Buffer Solution

Shoma Miyata[1], Mina Hoshino[1], Tasuku Isozaki[1], Takeshi Yamada[1], Hideyuki Sugimura[1], Yao–Zhong Xu[2], and Tadashi Suzuki[1]*

[1]*Department of Chemistry and Biological Science, Aoyama Gakuin University, 5–10–1 Fuchinobe, Chuo–ku, Sagamihara, Kanagawa 252–5258, Japan*
[2]*School of Life, Health and Chemical Sciences, The Open University, Milton Keynes MK7 6AA, United Kingdom*

ABSTRACT

2',3',5'–Tri–O–acetyl–6,8–dithioguanosine (taDTGuo) is a modified nucleoside of drug 6–thioguanine and further developed as a potential photochemotherapeutic agent due to its desirable properties of photosensitivity to UVA light and singlet molecular oxygen generation. The photochemical characteristics of taDTGuo under biological conditions (namely in aqueous solution) were intensively investigated by the steady–state absorption and emission, time–resolved near–infrared emission measurements, and quantum chemical calculations. taDTGuo was found to be held in sequential acid dissociation equilibria within pH 3.79–11.93. With the global fitting analysis of the absorption spectra at various pHs, two pK_a values of the equilibria were determined to be 7.02 ± 0.01 and 9.79 ± 0.01. Quantum chemical calculations suggested that its mono– and di–anionic species in the ground state should be 1–imide anionic form (N^1–taDTGuo$^-$) and 1,7–di–imide anionic form (taDTGuo^{2-}) respectively. taDTGuo generates singlet molecular oxygen effectively and has pH–dependent quantum yields. In conclusion, taDTGuo would be most useful as a potent agent for photochemotherapy under certain carcinomatous pH conditions.

1. INTRODUCTION

6–Thioguanine (6TG) is the pharmacologically active molecule derived from drugs azathioprine and mercaptopurine that have been widely prescribed for the treatment of cancers, leukemia, and autoimmune disease among others. [1–12] 6TG can be converted into its nucleoside, 6–thioguanosine [2–amino–9–(β–$_D$–ribofuranosyl) purine–6–thiol] (6TGuo), through cellular metabolism. 6TG localizing in tumor cell was reported to generate reactive oxygen species (ROS) when exposed to UVA light, thus inducing cellular apoptosis.[12] These findings indicate that 6TG and 6TGuo could be explore as an effective medical tool for cancer treatment due to their unique properties as photochemotherapeutic drugs like 4–thiothymidine,[13,14] including a photoactivatable genotoxic agent and a photosensitizer for photodynamic therapy (PDT), in addition to the hitherto known use as an anticancer medicine.

The photochemical characteristics of 6TG and 6TGuo have been studied by many investigators.[15–20] It has been reported that 6TGuo could generate $^1O_2{}^*$ effectively through the photosensitization reaction due to its dominant relaxation pathway of intersystem crossing from singlet excited state to triplet manifold, having a substantially long lifetime (above 1 µs).[15,16] Recently, to extend our understanding of the phototherapeutic ability of 6TG and 6TGuo, we designed and explored their tri–acetyl–protected thioguanosine derivatives, 2',3',5'–tri–O–acetyl–6–thioguanosine (ta6TGuo) and 2',3',5'–tri–O–acetyl–6,8–dithioguanosine (taDTGuo) (for chemical structures, see Scheme 1).[21] The solubilities of the acetylated derivatives in dehydrated organic solvents are much larger than the un–acetylated ones,[21,22] thus they are easier for handling because of their sufficient solubility in both aqueous and organic solvents, and they are still stable under physiological conditions. taDTGuo is of particular interest since it has the longest wavelength for absorption maximum and the highest value in terms of molar absorption coefficient among all thio–nucleobases and thio–nucleosides reported,[15–21,23–27] suggesting that taDTGuo would be much sensitive to the light penetrating into the human skin. In addition, taDTGuo as well as ta6TGuo can generate singlet molecular oxygen ($^1O_2{}^*$) effectively through a photosensitizing reaction. These results suggest that taDTGuo can be further developed as a potential agent for light–induced therapies.

The photochemical characteristics of taDTGuo under biological conditions (*i.e.* in aqueous solution) should be intensively investigated in order to develop taDTGuo as a photochemotherapeutic agent. In aqueous solution, native guanine (G), guanosine (Guo), 6TG, and 6TGuo were reported to be held in an acid dissociation equilibrium at 1–imide proton of the purine ring. The pK_a value at the 1–imide proton of guanosine was reported to be 9.25[28] whereas that of 6TGuo to be 8.35 $\pm$ 0.05,[29] indicating that the neutral and/or

anionic form should exist and be dependent on the surrounding pH condition. Certain microenvironments (*e.g.* pH condition) of tumor cells have been noted to be different from those of health cells.[30] To take advantage of these microenvironments, it is important to examine photophysical/photochemical processes for each species of these phototherapeutically useful thionucleosides.

In this article, firstly, we determine the pK_a values of taDTGuo (using the steady–state absorption spectra under various pH conditions) and assign the mono–anionic species of taDTGuo (from the Gibbs energy difference with aid of quantum chemical calculations). Secondly, we report its $\emptyset_\Delta$ values at various pHs (using time–resolved near–infrared emission measurement). We also discuss how these pK_a and pH–dependent $\emptyset_\Delta$ values could be used to help the thionucleoside be more effective for photochemotherapies.

2. EXPERIMENTAL METHODS

2.1 Chemicals and Steady–State Measurements.

Tri–acetyl–protected derivatives of taDTGuo, ta6TGuo, and taGuo were prepared as described in the previous report.[21] The structures of all synthesized products were characterized by ^{1}H NMR and their purities were estimated to be above 97% with a minor amount of impurity being H_2O. Phosphate buffer solution (pH 7.0) was used as a solvent. HCl(aq) and NaOH(aq) were used to adjust the pH value of the solvents, and the pH values were measured by a pH meter (TOA, HM–30G). The UV−vis absorption and emission spectra were recorded at room temperature with a spectrophotometer (JASCO, Ubest V–550) and a spectrofluorometer (JASCO, FP–6500), respectively.

2.2 Time–Resolved Near–Infrared Emission Spectroscopy.

Time–resolved near–infrared emission measurement was carried out with a thermoelectric cooled near–infrared photomultiplier tube (Hamamatsu Photonics, H10330–45; InP/InGaAsP, spectral response 950 to 1400 nm) combined with a longpass filter (Thorlabs, FEL1250; cut–on wavelength 1250 nm) and a bandpass filter (Edmund, Hard–coated bandpass filter; 1275 ± 50 nm). A XeCl excimer laser (COMPex 102; 308 nm, 120 mJ/pulse, 20 ns pulse duration, repetition rate 10 Hz) was used as an excitation light source. The sample solution flowed in a cell (Tosoh Quartz T514M−ES−10; 10 mm optical pass length) to avoid the contamination of photoproducts.

2.3 Quantum Chemical Calculations.

Ground− and excited−state calculations for corresponding purine bases [G (guanine),

6TG (6–thioguanine), DTG (6,8–dithioguanine) and their anionic species] were performed using the Gaussian 09W program package.[31] Ground−state geometries of the purine bases were optimized by the density functional theory (DFT) at the B3LYP/6−311+G(d,p) level. Vertical excitation energies were estimated by the time−dependent DFT (TD−DFT) at the TD−B3LYP/6−311+G(d,p) level. Solvent effects were modeled with the polarizable continuum model (PCM) for the ground− and excited−states. $S_1 \rightarrow S_0$ fluorescence spectra were simulated using the TD−DFT with the inclusions of Duschinsky and Herzberg−Teller contributions to the electronic transition dipole moments.[32]

3. RESULTS AND DISCUSSION

3.1 pH Dependence of Absorption Spectra in Aqueous Buffer Solution.

Absorption spectra of taDTGuo under various pH conditions are shown in Figure 1a. Spectral changes in the taDTGuo solutions were clearly observed along with the changing pH values, and the spectra of taDTGuo at higher pH value were found to exhibit blue−shifted absorption band. Figure 1a also shows several isosbestic points, of which two isosbestic points (at 356 nm and 350 nm) are most interesting as they are pH–dependent. The point at 356 nm was observed at pH 3.79~8.02 whereas the other at 350 nm was observed at pH 8.02~11.93. This reveals that three chemical species should be held in sequential equilibria due to two kinds of acid dissociations. The spectrum of taDTGuo at pH 3.79 agreed with that in acetonitrile solution,[21] indicating that the neutral form mainly exists under such an acidic condition whereas mono− and di−anionic species are under more basic conditions. Further discussion will be presented below.

The absorption spectra of taGuo and ta6TGuo in various pH aqueous solutions are shown in Figure 1b and 1c, respectively. pH–dependent spectral changes were also observed. In the case of taGuo, the characteristic absorption band with a maximum at 253 nm and a shoulder at around 275 nm were observed under a neutral condition, corresponding to its spectrum in acetonitrile solution.[21] The 253 nm band disappeared and a new band arose at around 270 nm along with the increasing pH values. The isosbestic point was observed at 278 nm. On the other hand, the spectra of ta6TGuo exhibited an isosbestic point at 327 nm and significantly blue−shifted absorption maxima from 342 nm to 319 nm by increasing the pH value of the solution, namely being more basic. No more spectral change in taGuo and ta6TGuo solutions was observed in the range of pH 4.0−7.42. Both species of taGuo and ta6TGuo exhibited a respective isosbestic point, suggesting that two chemical species were held in equilibrium due to acid

5

dissociation. This is consistent with the documented acid−base equilibrium for Guo and 6TGuo.[28,29] Thus, each of taGuo and ta6TGuo will have a single stable mono–anionic species whereas taDTGuo has two kinds of stable anionic species in the pH range examined.

3.2 Determination of pK_a.

As shown above, each of taGuo and ta6TGuo has a single equilibrium due to acid dissociation under the pH conditions examined. Then we determined the pK_a values of taGuo and ta6TGuo in their aqueous solutions from UV absorption spectra. The pK_a can be written down as follows:

$$pK_a = -pH + \log_{10}\frac{(D^{HA}-D)}{(D-D^{A^-})} \tag{1}$$

where D is the absorbance of the solution containing the mixture of the neutral species and the anionic species, D^{HA} and D^{A^-} are the absorbances of the neutral and the anionic species at the same concentration, respectively.[33,34] The plots of $\log_{10}\frac{(D^{HA}-D)}{(D-D^{A^-})}$ against the pH value were analyzed by using eq.1 (see Figure S1 in support information), and the pK_a values were estimated to be 9.53 ± 0.02 for taGuo and 8.41 ± 0.02 for ta6TGuo. These values well agreed with the reported ones for the 1−imide anion group (9.25 for Guo and 8.35 ± 0.05 for 6TGuo),[28,29] implying that there is no significant influence on acid dissociation at the 1−imide anion group by tri−acetyl protected ribose component. These results also confirm that the substitution of the carbonyl oxygen by a sulfur atom leads higher acid dissociation constant (K_a) at the 1−imide group.

Three chemical species should be held in equilibria due to sequential acid dissociations in taDTGuo aqueous solution. The pK_{a1} and pK_{a2} can be written as follows:

$$pK_{a1} = -\log_{10}\frac{[HA^-][H^+]}{[H_2A]} \tag{2}$$

$$pK_{a2} = -\log_{10}\frac{[A^{2-}][H^+]}{[HA^-]} \tag{3}$$

where, [H$_2$A], [HA$^-$], [A^{2-}] and [H$^+$] denote the concentrations of neutral, mono−anionic, di−anionic species, and protons, respectively. The total concentration of solutes, C_0, is written as follows.

$$C_0 = [\text{H}_2\text{A}] + [\text{HA}^-] + [\text{A}^{2-}] \tag{4}$$

From eqs. (2), (3), and (4), the concentrations for each species are written down.

$$[\text{H}_2\text{A}] = \frac{C_0}{1 + \frac{10^{-pK_{a1}}}{[\text{H}^+]} + \frac{10^{-(pK_{a1}+pK_{a2})}}{[\text{H}^+]^2}} \tag{5}$$

$$[\text{HA}^-] = \frac{C_0}{1 + \frac{[\text{H}^+]}{10^{-pK_{a1}}} + \frac{10^{-pK_{a2}}}{[\text{H}^+]}} \tag{6}$$

$$[\text{A}^{2-}] = \frac{C_0}{1 + \frac{[\text{H}^+]}{10^{-pK_{a2}}} + \frac{[\text{H}^+]^2}{10^{-(pK_{a1}+pK_{a2})}}} \tag{7}$$

The observed absorbance of the solution, D, is written down as:

$$D = \varepsilon^{\text{H}_2\text{A}}[\text{H}_2\text{A}] + \varepsilon^{\text{HA}^-}[\text{HA}^-] + \varepsilon^{\text{A}^{2-}}[\text{A}^{2-}] \tag{8}$$

where ε denotes the molar absorption coefficient. The ε is regarded as a function of wavelength, which can be described by linear combination of some gauss functions. Thus, a fitting function was written down as follows.

$$D(\lambda) = [\text{H}_2\text{A}]\left[\sum_i a_i exp\left\{-\left(\frac{\lambda-\lambda_i}{\Delta_i}\right)^2\right\}\right] + [\text{HA}^-]\left[\sum_j a_j exp\left\{-\left(\frac{\lambda-\lambda_j}{\Delta_j}\right)^2\right\}\right] +$$

$$[\text{A}^{2-}]\left[\sum_k a_k exp\left\{-\left(\frac{\lambda-\lambda_k}{\Delta_k}\right)^2\right\}\right] \tag{9}$$

The gauss function component of first and third terms on the right−hand side were known from the absorption spectra at pH 3.79 and pH 11.93 where only one species, either neutral or di−anionic species, exists. Using Eqs. (5), (6), (7), and (9) with pK_{a1}, pK_{a2}, a_j, λ_j and Δ_j as fitting parameters, global fitting analysis was carried out against the absorption spectra of taDTGuo at various pHs. Figure 2 shows the results of the global fitting analysis in the wavelength region from 310 to 420 nm (lower) and the residues of the analytic function (upper). Fitting curves well reproduced the absorption spectra, and the pK_{a1} and pK_{a2} were successfully determined to be 7.02 ± 0.01 and 9.79 ± 0.01, respectively. Figure 3 shows the absorption spectra of neutral, mono− and di−anionic species, obtained by the analysis.

3.3 Assignment of Anionic Species in Ground State.

taDTGuo was found to have three chemical species due to two stepwise dissociation equilibria. The deprotonation of taDTGuo can occur at the imide proton of 1− and/or 7−positions. It was reported that the deprotonation of 8−oxoguanosine, having two carbonyl groups at 6− and 8−positions of the purine ring, occurred firstly at the pyrimidine nitrogen (1−position) and secondly at the imidazole nitrogen (7−position) as the pH increased.[35–37] To identify structures of the deprotonated anionic species of taDTGuo, quantum chemical calculations were performed.

Optimized ground state geometries of 6,8−dithioguanine (DTG), 1−imide anionic form (N^1−DTG⁻), 7−imide anionic form (N^7−DTG⁻), and 1,7−diimide anionic form (DTG²⁻) are shown in Figure S2 (see supporting information). The bond lengths and the angles at the purine ring moiety were found to be comparable to each other. Almost all atoms of DTG lie in a plane of the purine ring except the amino protons (H^{12} and H^{13}) (for the atom labeling, see Scheme 1). The amino protons of anionic forms are largely out of the molecular plane. The $N^1C^2N^{11}H^{12}$ dihedral angle is 8.5° for DTG, 20.7° for N^1−DTG⁻, 22.8° for N^7−DTG⁻, and 23.9° for DTG²⁻. Similarly, the $N^1C^2N^{11}H^{13}$ dihedral angle is 174.7° for DTG, 160.3° for N^1−DTG⁻, 167.5° for N^7−DTG⁻, and 157.2° for DTG²⁻. Similar results were also observed on the 1−imide anionic form of G (G⁻) and 6TG (6TG⁻) (Figure S3). The $N^1C^2N^{11}H^{12}$ and the $N^1C^2N^{11}H^{13}$ dihedral angles of G⁻ and 6TG⁻ are out of the molecular plane by about 20°.

The polarizable continuum model (PCM) enables us to compute the Gibbs energy in implicit solvent, and Gibbs energy difference (ΔG) in solution can be estimated by

$$\Delta G = (G_{A^-} + G_{H^+}) - G_{HA} \tag{10}$$

where the G_{HA}, G_{A^-}, and G_{H^+} denote the Gibbs energy of neutral species, anionic species, and the proton in the aqueous solution, respectively.[38] The results calculated at PCM/6−311+G(d,p) are summarized in Table 1. The value of Gibbs energy difference in the ground state (ΔG_g) of N^1−DTG⁻ was clearly smaller than that of N^7−DTG⁻ (i.e. $\Delta G_g^{N^1-DTG^-} < \Delta G_g^{N^7-DTG^-}$), indicating that the former is readier for acid dissociation. Furthermore, in the S₁ state N^7−DTG⁻ was found to be more stable than N^1−DTG⁻ (i.e. $\Delta G_e^{N^1-DTG^-} > \Delta G_e^{N^7-DTG^-}$). Therefore the stable mono−anionic species generated by deprotonation of taDTGuo in the ground state should be 1−imide anionic form (N^1−taDTGuo⁻).

The ΔG_g value was also estimated by the acid dissociation constant obtained experimentally with the following equation,

8

$$\Delta G_g = -RT ln K_a \qquad\qquad (11)$$

where K_a, R, and T denote the dissociation equilibrium constant, the gas constant, and the absolute temperature, respectively. The ΔG_g values estimated from the K_a values are summarized in Table 1. The ΔG_g values of taGuo and ta6TGuo were close to their respective ΔG_g values estimated with the computational calculation of G and 6TG. The ΔG_g value of taDTGuo for the first step of deprotonation was close to the value estimated with the computational calculation of N^1-DTG^- in comparison with N^7-DTG^-. Thus, the stable mono−anionic species of taDTGuo in the ground state should be assigned to $N^1-taDTGuo^-$.

The absorption spectra of neutral, mono− and di−anionic species of taDTGuo, obtained by global fitting analysis, are shown in Figure 3a−3c. The calculated vertical transition energies and oscillator strengths of DTG, N^1-DTG^-, N^7-DTG^-, and DTG^{2-} are shown in Figure 3d. Computational results of DTG and DTG^{2-} well reproduced the absorption spectra of taDTGuo and di−anionic species, respectively. Thus, the di−anionic species of taDTGuo can be assigned to the 1,7−di−imide anion ($taDTGuo^{2-}$). The calculated vertical transition energies and oscillator strengths of N^1-DTG^- (but not of N^7-DTG^-) well reproduced the absorption spectrum of first step deprotonated species, further confirming that the most stable structure of mono−anionic species of taDTGuo at ground state is $N^1-taDTGuo^-$.

The absorption spectra of taGuo, ta6TGuo and their anionic species, and the calculated vertical transition energies and oscillator strengths of G, G^-, 6TG, and $6TG^-$ are shown in Figure S4. Computational results of G, G^-, 6TG, and $6TG^-$ also well reproduced the absorption spectra of their corresponding tri−acetyl protected nucleosides. Thus, the mono−anionic species of taGuo and ta6TGuo should be assigned to 1−imide anionic form of them, $taGuo^-$ and $ta6TGuo^-$, respectively.

Spectroscopic properties for singlet excited states of taDTGuo, taGuo, ta6TGuo, and their anionic species and computational values were listed in Table S1. The absorption maxima of the longest wavelength for taDTGuo, $N^1-taDTGuo^-$ and $taDTGuo^{2-}$ were assigned to the $S_1 \leftarrow S_0$ transition with $\pi\pi^*$ character.

The dissociation equilibria of taGuo, ta6TGuo, and taDTGuo in the ground state is described in Scheme 2. The first deprotonation of taDTGuo should occur at the 1−imide group ($pK_{a1} = 7.02 \pm 0.01$), followed by the second deprotonation at the 7−imide group ($pK_{a2} = 9.79 \pm 0.01$). The pK_a value for 1−imide group of taDTGuo (i.e 7.02 ± 0.01) was found to be smaller than that of ta6TGuo (i.e. 8.41). This reduced pK_a value can be

ascribed to the electron−withdrawing effect of the 8−thiocarbonyl group of taDTGuo.

3.4 Steady−State Emission Measurement and Franck−Condon Simulation.

Steady−state emission and excitation spectra of taDTGuo at pH 7.7 and 11.93 are shown in Figure 4a. The emission maxima were observed at 445 and 409 nm in the neutral (pH 7.7) and the most basic (pH 11.93) aqueous solution, respectively. Since the excitation spectrum at pH 11.93 (yellow broken line in Figure 4a) well corresponds to the absorption spectrum of taDTGuo^{2-} (see Figure 3c), the luminescent species at pH 11.93 can be attributed to be taDTGuo^{2-}. The excitation spectrum at pH 7.7 does not correspond to the absorption spectrum of N^1−taGuo$^-$, but it is similar to that of neutral taDTGuo. However, the emission intensity decreased as the solution became more acidic, and no emission was detected at pH 3.79. These results suggest that the luminescent species at pH 7.7 is not neutral taDTGuo.

To identify the luminescent species under neutral condition, S$_1$←S$_0$ fluorescence spectra of neutral DTG, N^1−DTG$^-$, N^7−DTG, and DTG^{2-} were simulated with the quantum chemical calculation (Figure 4b). The simulated spectrum of DTG^{2-} well reproduced the observed fluorescence spectrum at pH 11.93. The experimental emission spectrum at pH 7.7 has the accordance with the computational spectrum of N^7−DTG$^-$. However, N^7−taDTGuo would not be populated in the ground state, as discussed above. This indicates that N^7−taDTGuo is generated from neutral taDTGuo due to acid dissociation in the excited state, followed by yielding fluorescence, as described in Scheme 3. Computational ΔG value for singlet excited state of N^7−taDTGuo$^-$ was found to be smaller than that for N^1−taDTGuo$^-$ (as listed in Table 1), suggesting to the generation of N^7−taDTGuo$^-$ by excitation of neutral taDTGuo at around pH 7.0. It is interesting to discuss on the isotope effect on the equilibria in both ground and excited states, especially on the excited state dynamics. Thus, nano- and femto-second spectroscopies on the excited states are under way.

Generally, thio−analogues of nucleobases and nucleosides are known to be non−fluorescent due to their dominant relaxation pathway to the triplet manifold (i.e. intersystem crossing).[15,16,23−27] This is the first report that an anionic species of thio−analogues, such as taDTGuo, can be luminescent and that the excited state characteristics of the anionic species can be quite different from its neutral species, implying the ability for generating singlet molecular oxygen (^{1}O$_2$*) would be individual for each species.

3.5 Quantum Yields of Singlet Oxygen Generation of Thio−substituted Guanosines in Aqueous Buffer Solutions.

10

To obtain the $\varnothing_\Delta^{obs}$ values for taDTGuo at various pHs, the time−resolved near−infrared emission measurements were carried out. In these measurements, both neutral and anionic species of taDTGuo were excited simultaneously at excitation laser wavelength (308 nm) in aqueous solutions. Figure 5a shows the time–profile of singlet molecular oxygen phosphorescence produced through photosensitization by taDTGuo in oxygen−saturated aqueous solutions at various pHs. The decaying signals were fitted with a single−exponential function and their lifetimes were determined to be about 3.5 microsecond, which well agrees with the lifetime of $^1O_2{}^*$ in H_2O.[39] The spike–like emission immediately after laser irradiation are due to the scattered laser light or fluorescence of the solutions.

The quantum yields of $^1O_2{}^*$ generation by taDTGuo at various pHs were determined in O_2 saturated aqueous solutions relative to optically matched methylene blue (MB) solution ($\varnothing_\Delta = 0.39$ at pH 7.4).[40] Individual longer−lived phosphorescence traces in the time domain after 2.5 μs were fitted by using a single–exponential function to estimate the emission intensity maxima immediately after laser irradiation ($I_S{}^0$). The $I_S{}^0$ value was plotted against the laser fluence (I_L) (Figure 5b), showing a good linear relationship between $I_S{}^0$ and I_L. The values of the slope obtained from these plots ($I_S{}^0 / I_L$) were plotted against the ground state absorptance at excitation wavelength ($1–10^{-A}$), as shown in Figure 5c. These plots also show good linear relationships. By comparing the slopes of taDTGuo at various pHs with that of MB at pH 7.4, $\varnothing_\Delta^{obs}$ values were determined.

Table 2 lists the results and figure 6a shows the plots of $\varnothing_\Delta^{obs}$ value against pH value of the solution. The $\varnothing_\Delta^{obs}$ value clearly depends on the pH of the solution, and the distribution of the $\varnothing_\Delta^{obs}$ is also clearly correlated with the concentration ratio of neutral taDTGuo, N^1−taDTGuo$^-$ and taDTGuo^{2-} as shown in Figure 6b. The quantum yield of $^1O_2{}^*$ generation of neutral taDTGuo (0.32 ± 0.01) is found to be larger than that of taDTGuo^{2-} (0.25 ± 0.01) (see Table 3). Figure 6a also shows that $\varnothing_\Delta^{obs}$ value was minimized at pH 8.4, indicating that quantum yield of singlet oxygen generation by N^1−taDTGuo$^-$ (the main species at pH 8.4) should be the smallest. As $\varnothing_\Delta^{obs}$ can be described with linear−combination of the product of quantum yields of each species and the absorbance,

$$\varnothing_\Delta^{obs} = \frac{1}{A_{ex}} \left(\varepsilon_{ex}^{H_2A} \cdot [H_2A] \cdot \varnothing_\Delta^{H_2A} + \varepsilon_{ex}^{HA^-} \cdot [HA^-] \cdot \varnothing_\Delta^{HA^-} + \varepsilon_{ex}^{A^{2-}} \cdot [A^{2-}] \cdot \varnothing_\Delta^{A^{2-}} \right) \quad (12)$$

where A_{ex}, ε_{ex} denote the absorbance and a molar absorption coefficient at excitation wavelength (308 nm) respectively, so we tried to estimate the quantum yield of $^1O_2{}^*$

generation by N^1−taDTGuo$^-$ with eq. (12). The analysis curve well represented the distribution curve of the $\emptyset_\Delta^{obs}$ plots, and the quantum yield of $^1O_2{}^*$ generation for N^1−taDTGuo$^-$, $\emptyset_\Delta^{HA^-}$, was successfully determined to be 0.17 ± 0.02.

According to the analysis curve in Figure 6a, the $\emptyset_\Delta^{obs}$ will sharply decline at pH greater than around 6 and become minimal at pH 8.6. The microenvironment of tumor cells is known to be slightly acidic than that of normal cells, and pH values are reported to be around 6−7 for some of tumor cells and above 7.0 for normal cells.[30] Thus, the pH sensitivity of taDTGuo should be considered when using as a phototherapeutic sensitizer for the treatment of tumor cells.

The $\emptyset_\Delta$ values for ta6TGuo and ta6TGuo$^-$ were also determined. However, the difference in the value for ta6TGuo and ta6TGuo$^-$ was small, indicating their excited state dynamics would be similar to each other. In taGuo and taGuo$^-$ solutions, no near–infrared emission was detected. This is because the dominant relaxation pathway from excited singlet state of un–thiolated (native) guanine is known to be ultrafast internal conversion to the ground state,[41] resulting few generation of $^1O_2{}^*$.

The $\emptyset_\Delta$ values of neutral taDTGuo, N^1−taDTGuo$^-$ and taDTGuo^{2-} are different, as listed in Table 3. $^1O_2{}^*$ is considered to generate through energy transfer from the T_1 state of a donor molecule to an oxygen molecule ($X^3\Sigma_g^-$) as an energy acceptor by collision, thus the $\emptyset_\Delta$ value should depend on the following factors: the intersystem crossing quantum yield, the triplet lifetime of the sensitizer, and the S_Δ value (a fraction of the triplet states quenched by dissolved oxygen which gives rise to singlet oxygen formation). Generally, a triplet state having $\pi\pi^*$ character has been reported to give a S_Δ value within the range of 0.7–1.0, whereas it is ~0.3 for an $n\pi^*$ triplet state.[42] Each of the T_1 state of neutral taDTGuo, N^1−taDTGuo$^-$ and taDTGuo^{2-} can be assigned to the $\pi\pi^*$ state by the TD–DFT calculation. The T_1 state energies were estimated from the vertical transition energies to the T_1 state, as listed in Table 3. The T_1 state energies of all species are large enough to surpass vertical transition energy of oxygen molecules (0.97 eV; $a^1\Delta_g \leftarrow X^3\Sigma_g^-$).[40] Therefore, the differences in $\emptyset_\Delta$ will result from the triplet lifetime of each species and/or quantum yield of intersystem crossing to triplet manifolds. The lifetimes of taDTGuo and taDTGuo^{2-} have been initially estimated to be several microseconds, ten times longer than that of N^1−taDTGuo$^-$. These details would be very valuable when developing and optimizing thionucleosides (including taDTGuo) as phototherapeutic agents. On the other hand, triplet lifetime was largely affected by the concentration of the parent molecule (self–quenching), and the quenching rate constant of the triplet by oxygen molecule has not been obtained yet. So, to gain the more detailed information on the triplet state for each species, time–resolved absorption spectroscopy would be an ideal

approach and is now under way.

4. CONCLUSION

taDTGuo is a modified nucleoside of pharmacological active drug 6–thioguanine. The steady–state absorption measurements were carried out to clarify its absorption characteristics and to determine its pK_a values. The absorption spectra were found to be pH–dependent. taDTGuo was also noted to be held in sequential equilibria and its pK_{a1} and pK_{a2} were determined to be 7.02 ± 0.01 and 9.79 ± 0.01 respectively by global fitting analysis for the absorption spectra. First– and second–deprotonated species of taDTGuo were attributed to 1–imide anionic form (N^1–taDTGuo$^-$) and di–imide anionic form (taDTGuo^{2-}) respectively by comparing each of the absorption spectra with its corresponding oscillator strengths, vertical transition energies, and Gibbs energy differences obtained from quantum chemical calculations. Steady–state emission measurements revealed that N^7–taDTGuo$^-$, being less stability than N^1–taDTGuo$^-$ at ground states, was only generated at singlet excited state of neutral taDTGuo under near neutral aqueous solution. Time–resolved near–infrared emission measurements were used to determine the $\emptyset_\Delta$ of taDTGuo and found that the $\emptyset_\Delta$ value was also pH–dependent due to the concentration ratio in sequential equilibria of neutral taDTGuo, N^1–taDTGuo$^-$ and taDTGuo^{2-}, thus taDTGuo could be used as a pH–sensitive phototherapeutic sensitizer to treat tumor cells. Each $\emptyset_\Delta$ was successfully determined to be 0.32 ± 0.01 for neutral taDTGuo, 0.17 ± 0.02 for N^1–taDTGuo$^-$ and 0.25 ± 0.01 for taDTGuo^{2-}. These different values in $\emptyset_\Delta$ result from the triplet lifetime of each species and/or quantum yield of intersystem crossing to triplet manifolds. The pH–dependent $\emptyset_\Delta$ values and the pK_a values, reported here, should provide useful information regarding which species of the thionucleoside would be most effective for photochemotherapies.

ASSOCIATED CONTENT

Supporting Information

(1) Spectroscopic properties for singlet excited states of taDTGuo, taGuo, ta6TGuo, and their anionic species and calculated values obtained at PCM/TD-B3LYP/6-311+G(d,p) level. (2) Plots of $\log_{10} \frac{\left(D^{HA}-D\right)}{\left(D-D^{A^-}\right)}$ *vs*. pH for taGuo (black) and ta6TGuo (red).

(3) Optimized structures at the ground state of DTG, N^1–DTG$^-$, N^7–DTG$^-$, and DTG^{2-}.

(4) Optimized structures at the ground state of 6TG, 6TG⁻, G, and G⁻.

(5) (a) Absorption spectra of taGuo and its anionic species, and oscillator strength and vertical transition energies of G and G⁻. (b) Absorption spectra of ta6TGuo and its anionic species, and oscillator strength and vertical transition energies of 6TG and 6TG⁻.

REFERENCES

(1) Daehn, I.; Brem, R.; Barkauskaite, E.; Karran, P. 6−Thioguanine Damages Mitochondrial DNA and Causes Mitochondrial Dysfunction in Human Cells. *FEBS Letters* **2011**, *585*, 3941−3946.

(2) Zhang, X.; Jeffs, G.; Ren, X.; O'Donovan, P.; Montaner, B.; Perrett, C. M.; Karran, P.; Xu, Y.−Z. Novel DNA Lesions Generated by the Interaction Between Therapeutic Thiopurines and UVA Light. *DNA Repair* **2007**, *6*, 344−354.

(3) Zou, X.; Zhao, H.; Yu, Y.; Su, H. Formation of Guanine−6−sulfonate from 6‑Thioguanine and Singlet Oxygen: A Combined Theoretical and Experimental Study. *J. Am. Chem. Soc.* **2013**, *135*, 4509−4515.

(4) Ren, X.; Xu, Y−Z.; Karran, P. Photo−oxidation of 6−Thioguanine by UVA: The Formation of Addition Products with Low Molecular Weight Thiol Compounds. *Photochem. Photobiol.* **2010**, *86*, 1038−1045.

(5) Ren, X.; Li, F.; Jeffs, G.; Zhang, X.; Xu, Y−Z.; Karran, P. Guanine Sulphinate is a Major Stable Product of Photochemical Oxidation of DNA 6−Thioguanine by UVA Irradiation. *Nucleic Acids Res*. **2010**, *38*, 1832−1840.

(6) Lapage, G. A. Incorporation of 6−Thioguanine into Nucleic Acids. *Cancer Res.* **1960**, *20*, 403−408.

(7) Rubin, Y. V.; Blagoi, Y. P.; Bokovoy, V. A. 6−Thioguanine Luminescence Probe to Study DNA and Low−Molecular−Weight Systems. *J. Fluores.* **1995**, *5*, 263−272.

(8) Qu, P.; Lu, H.; Ding, X.; Tao, Y.; Lu, Z. Influences of Urea and Guanidine Hydrochloride on the Interaction of 6−Thioguanine with Bovine Serum Albumin. *Spectros. Acta A* **2009**, *74*, 1224−1228.

(9) Massey, A.; Xu, Y.−Z.; Karran, P. Photoactivation of DNA Thiobases as a Potential Novel Therapeutic Option. *Curr. Biol.* **2001**, *11*, 1142−1146.

(10) Brem, R.; Li, F.; Karran, P. Reactive Oxygen Species Generated by Thiopurine/ UVA Cause Irreparable Transcription−Blocking DNA Lesions. *Nucleic Acids Res.* **2009**, *37*, 1951−1961.

(11) Lepage, G. A.; Jones, M. Further Studies on the Mechanism of Action of 6−Thioguanine. *Cancer Res.* **1961**, *21*, 1590−1594.

(12) O'Donovan, P.; Perrett, C. M.; Zhang, X.; Montaner, B.; Xu, Y−Z.; Harwood, C. A.;

McGregor, J. M.; Walker, S. L.; Hanaoka, F.; Karran, P. Azathioprine and UVA Light Generate Mutagenic Oxidative DNA Damage. *Science* **2005**, *309*, 1871−1874.

(13) Pridgeon, S. W.; Heer, R.; Taylor, G.A.; Newell, D. R.; O'Toole, K.; Robinson, M.; Xu, Y−Z.; Karran, P.; Boddy, A. V. Thiothymidine Combined with UVA as a Potential Novel Therapy for Bladder Cancer. *Br. J. Cancer* **2011**, *104*, 1869−1876.

(14) Reelfs O.; Karran, P.; Young, A. R. 4−Thiothymidine Sensitization of DNA to UVA Offers Potential for a Novel Photochemotherapy. *Photochem. Photobiol. Sci.* **2012**, *11*, 148−154.

(15) Reichardt, C.; Guo, C.; Crespo−Hernández, C. E. Excited−State Dynamics in 6−Thioguanosine from the Femtosecond to Microsecond Time Scale. *J. Phys. Chem. B* **2011**, *115*, 3263−3270.

(16) Pollum, M.; Ortiz−Rodríguez, L. A.; Jockusch, S.; Crespo−Hernández, C. E. The Triplet State of 6−Thio−2'−deoxyguanosine: Intrinsic Properties and Reactivity Toward Molecular Oxygen. *Photochem. Photobiol.* **2016**, *92*, 286−292.

(17) Ashwood, B.; Jockusch, S.; Crespo−Hernández, C. E. Excited−State Dynamics of the Thiopurine Prodrug 6−Thioguanine: Can N9−Glycosylation Affect Its Phototoxic Activity? *Molecules* **2017**, *22*, 379−393.

(18) Rubin, Y. V. Physical Properties of Anticancer Drug 6−Thioguanine. *Proceedings of SPIE−The International Society for Optical Engineering* **2004**, *5507*, 346−357.

(19) Siouri, F. M.; Boldissar, S.; Berenbeim, J. A.; De Vries, M. S. Excited State Dynamics of 6−Thioguanine. *J. Phys. Chem. A* **2017**, *121*, 5257−5266.

(20) Zhang, Y.; Zhu, X.; Smith, J.; Haygood, M. T.; Gao, R. Direct Observation and Quantitative Characterization of Singlet Oxygen in Aqueous Solution upon UVA Excitation of 6−Thioguanines. *J. Phys. Chem. B* **2011**, *115*, 1889−1894.

(21) Miyata, S.; Yamada, T.; Isozaki, T.; Sugimura, H.; Xu, Y−Z.; Suzuki, T. Absorption Characteristics and Quantum Yields of Singlet Oxygen Generation of Thioguanosine Derivatives. *Photochem. Photobiol*, in press.

(22) Lewis, L. R.; Robins, R. K.; Cheng, C. C. The Preparation and Antitumor Properties of Acylated Derivatives of 6−Thiopurine Ribosides. *J. Med. Chem.* **1964**, *7,* 200−204.

(23) Harada, H.; Suzuki, T.; Ichimura, T.; Xu, Y−Z. Triplet Formation of 4−Thiothymidine and Its Photosensitization to Oxygen Studied by Time−Resolved Thermal Lensing Technique. *J. Phys. Chem. B* **2007**, *111*, 5518−5524.

(24) Kuramochi, H.; Kobayashi, T.; Suzuki, T.; Ichimura, T. Excited−State Dynamics of 6−Aza−2−thiothymine and 2−Thiothymine: Highly Efficient Intersystem Crossing and Singlet Oxygen Photosensitization. *J. Phys. Chem. B* **2010**, *114*, 8782−8789.

(25) Harada, Y.; Okabe, C.; Kobayashi, T.; Suzuki, T.; Ichimura, T.; Nishi, N.; Xu, Y−Z.

Ultrafast Intersystem Crossing of 4−Thiothymidine in Aqueous Solution. *J. Phys. Chem. Lett.* **2010**, *1*, 480−484.

(26) Pollum, M.; Jockusch, S.; Crespo−Hernández, C. E. Increase in the Photoreactivity of Uracil Derivatives by Doubling Thionation. *Phys. Chem. Chem. Phys.* **2015**, *17*, 27851−27861.

(27) Pollum, M.; Jockusch, S.; Crespo−Hernández, C. E. 2,4−Dithiothymine as a Potent UVA Chemotherapeutic Agent. *J. Am. Chem. Soc.* **2014**, *136*, 17930−17933.

(28) Izatt, R. M.; Christensen, J. J.; Rytting, J. H. Sites and Thermodynamic Quantities Associated with Proton and Metal Ion Interaction with Ribonucleic Acid, Deoxyribonucleic Acid, and Their Constituent Bases, Nucleosides, and Nucleotides. *Chem. Res.* **1971**, *71*, 439−482.

(29) Fox, J. J.; Wempen, I.; Hampton, A.; Doerr, I. L. Thiation of Nucleosides. I. Synthesis of 2−Amino−6−mercapto−9−/3−D−ribofuranosylpurine ("Thioguanosine") and Related Purine Nucleosides. *J. Am. Chem. Soc.* **1958**, *80*, 1669–1675.

(30) Gillies, R. J.; Raghunand, N.; Karczmar, G. S.; Bhujwalla, Z. M. MRI of the Tumor Microenvironment. *J. Magn. Reson. Imaging* **2002**, *16*, 430−450.

(31) Gaussian 09, Revision D.01, Frisch, M. J.; Trucks, G. W.; Schlegel, H. B.; Scuseria, G. E.; Robb, M. A.; Cheeseman, J. R.; Scalmani, G.; Barone, V.; Mennucci, B.; Petersson, G. A. ; Nakatsuji, H.; Caricato, M.; Li, X. ; Hratchian, H. P.; Izmaylov, A. F.; Bloino, J.; Zheng, G.; Sonnenberg, J. L.; Hada, M.; Ehara, M.; Toyota, K.; Fukuda, R.; Hasegawa, J.; Ishida, M.; Nakajima, T.; Honda, Y.; Kitao, O.; Nakai, H.; Vreven, T.; Montgomery, J. A.; Peralta, Jr., J. E.; Ogliaro, F.; Bearpark, M.; Heyd, J. J.; Brothers, E.; Kudin, K. N.; Staroverov, V. N.; Keith, T.; Kobayashi, R.; Normand, J.; Raghavachari, K.; Rendell, A.; Burant, J. C.; Iyengar, S. S.; Tomasi, J.; Cossi, M.; Rega, N.; Millam, J. M.; Klene, M.; Knox, J. E.; Cross, J. B.; Bakken, V.; Adamo, C.; Jaramillo, J.; Gomperts, R.; Stratmann, R. E. ; Yazyev, O.; Austin, A. J.; Cammi, R.; Pomelli, C.; Ochterski, J. W.; Martin, R. L.; Morokuma, K.; Zakrzewski, V. G.; Voth, G. A.; Salvador, P.; Dannenberg, J. J.; Dapprich, S.; Daniels, A. D.; Farkas, O.; Foresman, J. B.; Ortiz, J. V.; Cioslowski J.; Fox, D. J. Gaussian, Inc., Wallingford CT, **2013**.

(32) Barone, V.; Bloino, J.; Biczysko, M. Vibrationally−Resolved Electronic Spectra in GAUSSIAN 09. *GAUSSIAN 09 Revision A.02*, **2010**.

(33) Patterson, G. S. A Simplified Method for Finding the pK_a of an Acid–Base Indicator by Spectrophotometry. *J. Chem. Educ.* **1999**, *76*, 395−398.

(34) Salgado, L. E. V; Vargas−Hernández, C. Spectrophotometric Determination of the pK_a, Isosbestic Point and Equation of Absorbance vs. pH for a Universal pH Indicator.

Am. J. Anal. Chem. **2014**, *5*, 1290−1301.

(35) Verdolino, V.; Cammi, R.; Munk, B. H.; Schlegel, H. B. Calculation of pKa Values of Nucleobases and the Guanine Oxidation Products Guanidinohydantoin and Spiroiminodihydantoin using Density Functional Theory and a Polarizable Continuum Model. *J. Phys. Chem. B* **2008**, *112*, 16860−16873.

(36) Zhang, Y.; Dood, J.; Beckstead, A.; Chen, J.; Li, X−B.; Burrows, C. J.; Lu, Z.; Matsika, S.; Kohler, B. *J. Phys. Chem. A* **2013**, *117*, 12851−12857.

(37) Sandra, J. C.; Bongsup, P. C.; Fred, F. K.; Frederick, E. E. Structural and Conformational Analyses of 8−Hydroxy−2'−deoxyguanosine. *Chem. Res. Toxicol.* **1989**, *2*, 416−422.

(38) Matsui, T.; Oshiyama, A.; Shigeta, Y. A Simple Scheme for Estimating the pK_a Values of 5−Substituted Uracils. *Chem. Phys. Lett.* **2011**, *502*, 248−252.

(39) Rodgers, M. A. J. Solvent–Induced Deactivation of Singlet Oxygen: Additivity Relationships in Nonaromatic Solvents. *J. Am. Chem. Soc.* **1983**, *105*, 6201−6205.

(40) Wilkinson, F.; Helman, W. P.; Ross, A. B. Quantum Yields for the Photosensitized Formation of the Lowest Electronically Excited Singlet State of Molecular Oxygen in Solution. *J. Phys. Chem. Ref. Data,* **1993**, *22*, 113−262.

(41) Barbatti, M.; Borin, A. C.; Ullrich, S. Photoinduced Processes in Nucleic Acids. *Top. Curr. Chem.* **2015**, *335*, 1−32.

(42) Schweitzer, C.; Schmidt, R. Physical Mechanisms of Generation and Deactivation of Singlet Oxygen. *Chem. Rev.* **2003**, *103*, 1685−1758.

Table 1. Acidity Constants and Experimental and Computational Dissociation Energies.

	Experimental			Theoretical		
	pK_a [a]	K_a [b]	ΔG_g [c] / kcal mol^{-1}	Species [d]	ΔG_g [e] / kcal mol^{-1}	ΔG_e [f] / kcal mol^{-1}
taDTGuo	7.02 ± 0.01	9.55×10^{-8}	9.58	N^1–DTG$^-$	**11.81**	16.36
				N^7–DTG$^-$	14.54	**10.57**
	9.79 ± 0.01	1.62×10^{-10}	22.9	DTG^{2-}	33.36	38.29
taGuo	9.53 ± 0.02 (9.25) [g]	2.95×10^{-10}	13.0	G$^-$	19.88	
ta6TGuo	8.41 ± 0.02 (8.35 ± 0.05) [h]	3.89×10^{-9}	11.5	6TG$^-$	14.80	

[a] Determined by fitting analysis using eqs. (1), (5), (6), (7) and (9). [b] Acid dissociation constant. [c] Dissociation energy estimated by using eq. (11). [d] Corresponding anionic species of nucleobases, 1–imide anionic form of 6,8–dithioguanine (N^1–DTG$^-$), 7–imide anionic form of 6,8–dithioguanine (N^7–DTG$^-$), 1,7–diimide anionic form of 6,8–dithioguanine (DTG^{2-}), 1–imide anionic form of guanine (G$^-$) and 1–imide anionic form of 6–thioguanine (6TG). [e] Gibbs energy difference for anionic species from neutral form in the ground state and [f] that in the singlet excited state estimated by using eq. (10). Gibbs energies of each species and proton were calculated at the PCM/B3LYP/6–311+G(d,p) or the PCM/TD–B3LYP/6–311+G(d,p) level, and obtained from reported value (–270.01 kcal mol^{-1})[38], respectively. [g] Reported value in the ref 28. [h] Reported value in the ref 29.

Table 2. Apparent Quantum Yield of Singlet Oxygen Generation for taDTGuo at Various pHs.

| pH	$\emptyset_\Delta^{obs}$
4.0	0.32 ± 0.01
6.4	0.31 ± 0.01
7.4	0.21 ± 0.01
8.4	0.18 ± 0.01
10.0	0.21 ± 0.01
12.0	0.25 ± 0.01

Table 3. Quantum Yield of Singlet Oxygen Generation and Triplet Energies for taDTGuo, ta6TGuo and Their Anionic Species.

	$\emptyset_\Delta$ [a]	E_T [b] / eV
taDTGuo	0.32 ± 0.01	2.44
N^1-taDTGuo$^-$	0.17 ± 0.02	2.81
taDTGuo^{2-}	0.25 ± 0.01	2.79
ta6TGuo	0.34 ± 0.01	2.71
ta6TGuo$^-$	0.30 ± 0.01	2.98

[a] Extracted quantum yields of singlet oxygen generation for taDTGuo, ta6TGuo and their anionic species. [b] Triplet state energy calculated at the PCM/TD–B3LYP/6–311+G(d,p) level.
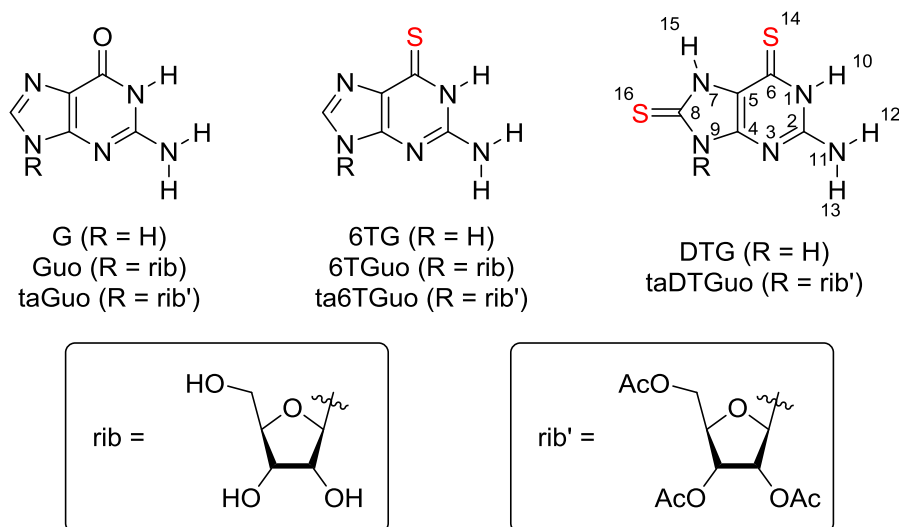
Scheme 1. Structures of guanine, thioguanines, and their nucleosides.
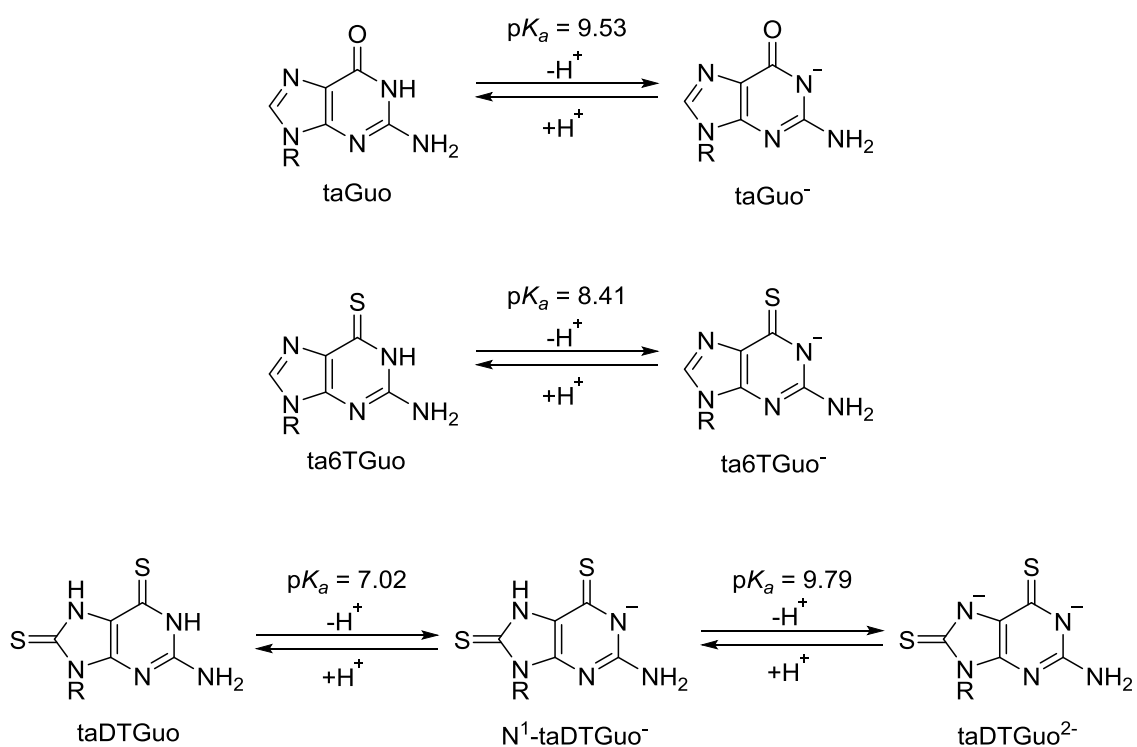
Scheme 2. Major dissociation equilibria and site–specific pK_a of taGuo, ta6TGuo, and taDTGuo.
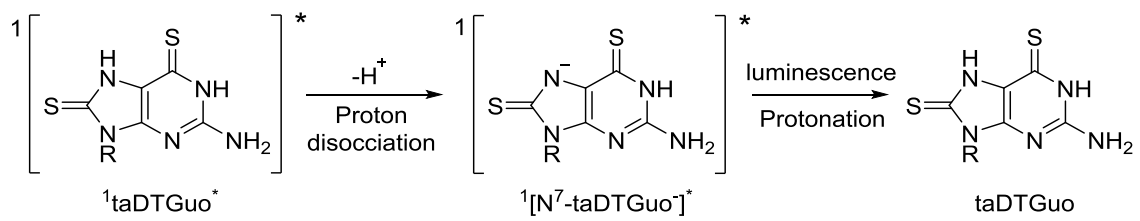
Scheme 3. Projection of radiative process from singlet excited state of taDTGuo under a nearly neutral pH condition.

FIGURE CAPTIONS

Figure 1. Absorption spectra of (a) taDTGuo (9.31 µM), (b) taGuo (32.0 µM), and (c) ta6TGuo (10.0 µM) in phosphate buffer solutions at various pHs.

Figure 2. The absorption spectra of taDTGuo at pH (colored broken lines), the analysis curve of best global fitting (black lines), and residues of the analytic function (upper in the figure). The resultant fitting curves are almost identical to the experimental spectra.

Figure 3. (a) Absorption spectrum of neutral taDTGuo. (b) Absorption spectrum of mono–anionic species of taDTGuo obtained by global fitting analysis. (c) Absorption spectrum of di–anionic species. (d) Calculated vertical transition energies and oscillator strength of neutral 6,8–dithioguanine (DTG) (red bars), 1–imide anionic form of 6,8–dithioguanine (N^1-DTG^-) (blue bars), 7–imide anionic form of 6,8–dithioguanine (N^7-DTG^-) (yellow bars), and 1,7–diimide anionic form of 6,8–dithioguanine (DTG^{2-}) (green bars) at PCM/TD–B3LYP/6–311+G(d,p) level.

Figure 4. (a) Steady–state emission spectra after excitation at 270 nm of taDTGuo at pH 7.7 (yellow solid line) and 11.93 (green solid line), and excitation spectra recorded using λ_{em} = 480 nm at pH 7.7 (yellow broken line) and λ_{em} = 450 nm at pH 11.93 (green broken line). (b) Franck–Condon simulation for fluorescence spectrum of DTG (red solid line), N^1-DTG^- (blue solid line), N^7-DTG^- (yellow solid line) and DTG^{2-} (green solid line) resulted by $S_1 \rightarrow S_0$ transitions.

Figure 5. (a) Decay profiles of singlet oxygen phosphorescence measured at around 1275 nm of taDTGuo and MB at various pHs. Signals are corrected for absorptance at excitation wavelength (308 nm) and incident laser power. (b) Plots of the emission intensity maxima (I_S^0) immediately after laser irradiation in taDTGuo solutions at pH 4.0 against incident laser power (I_L), and (c) plots of the I_S^0/I_L value of taDTGuo and MB against the absorptance ($1-10^{-A}$) at excitation wavelength (308 nm).

Figure 6. (a) The plots of $\emptyset_\Delta^{obs}$ as a function of proton concentration in taDTGuo solution and analysis curve. (b) The pH–dependent abundance ratio of taDTGuo (red), N^1–taDTGuo$^-$ (blue) and taDTGuo^{2-} (green).
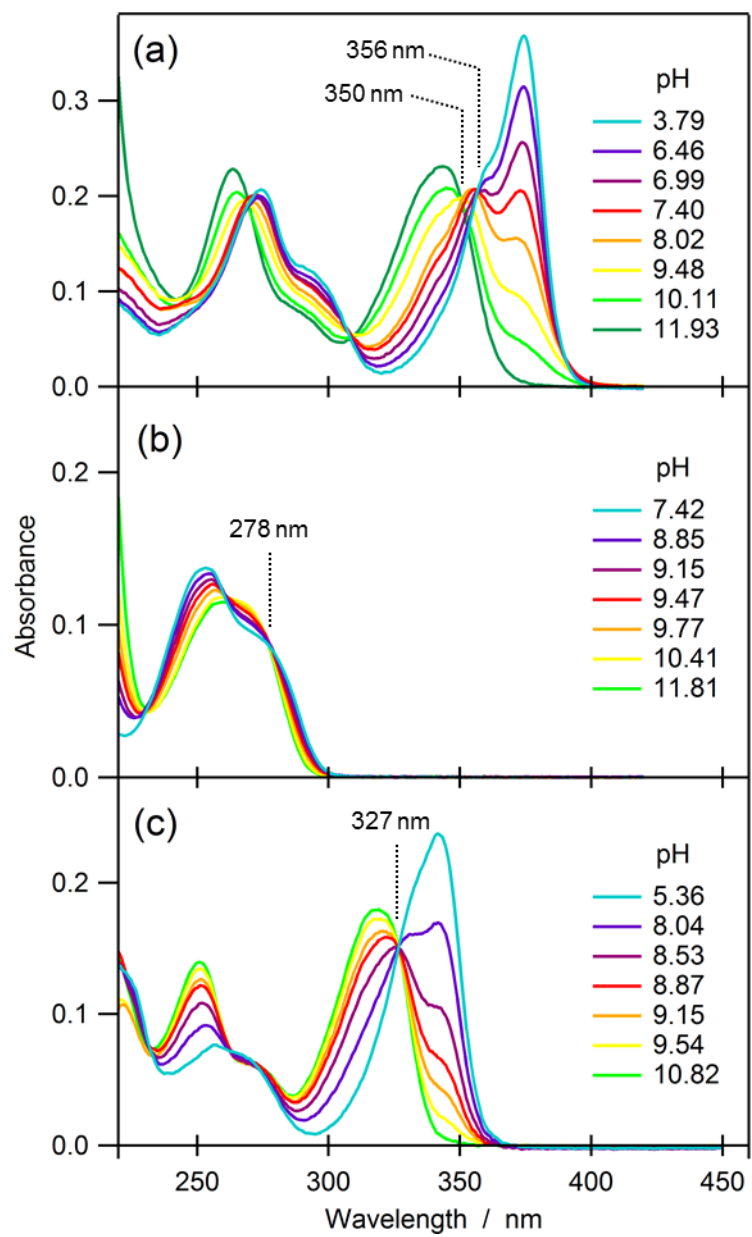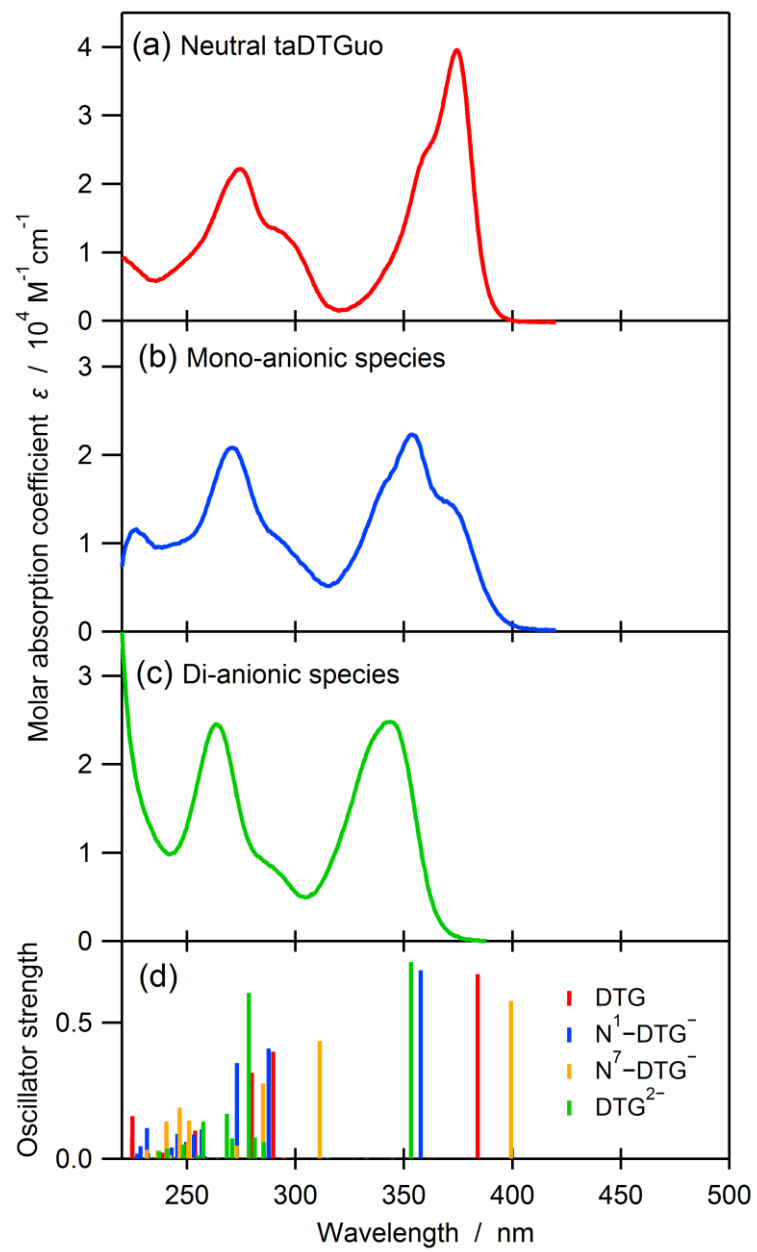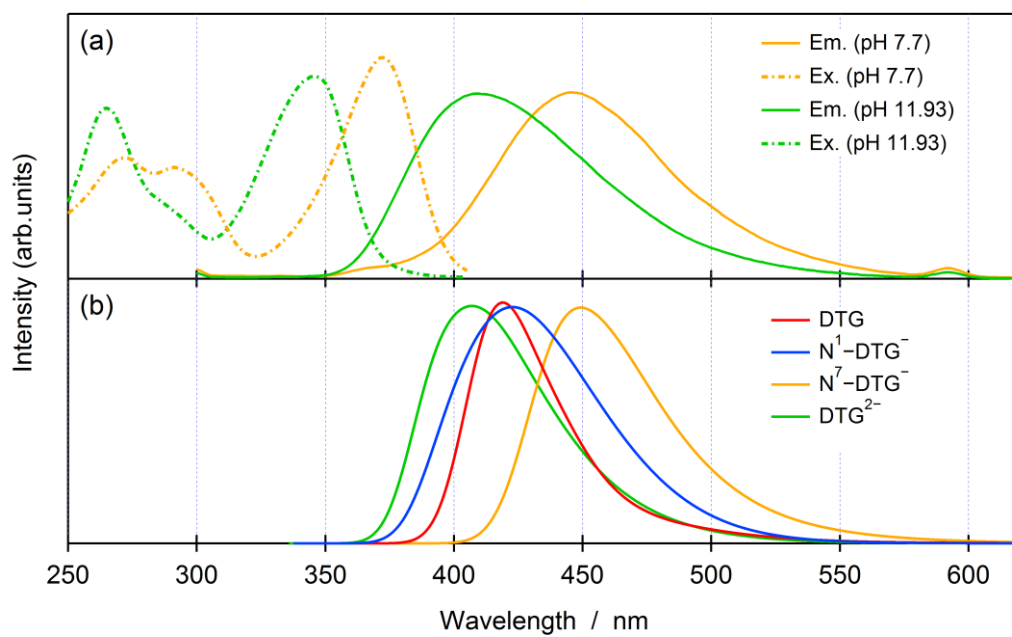
Figure 1. S. Miyata *et al*.
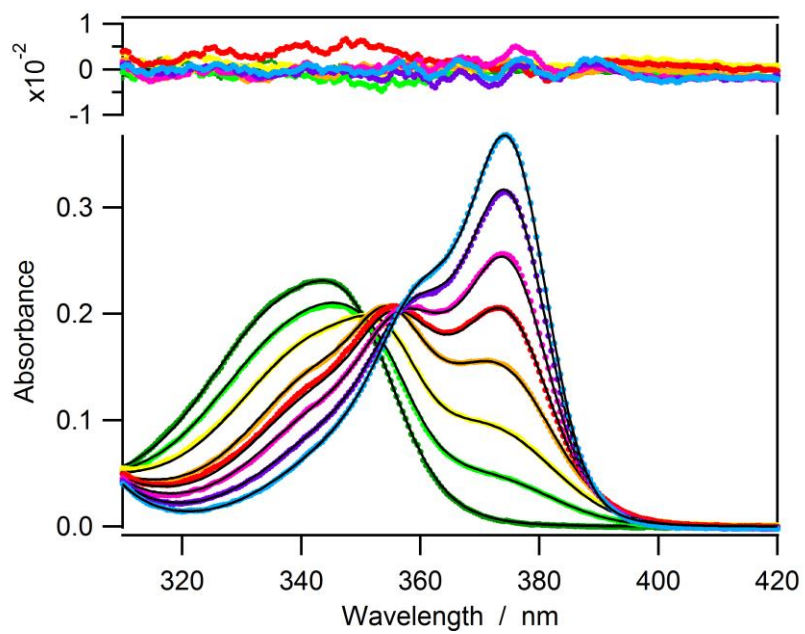
Figure 2. S. Miyata *et al*.

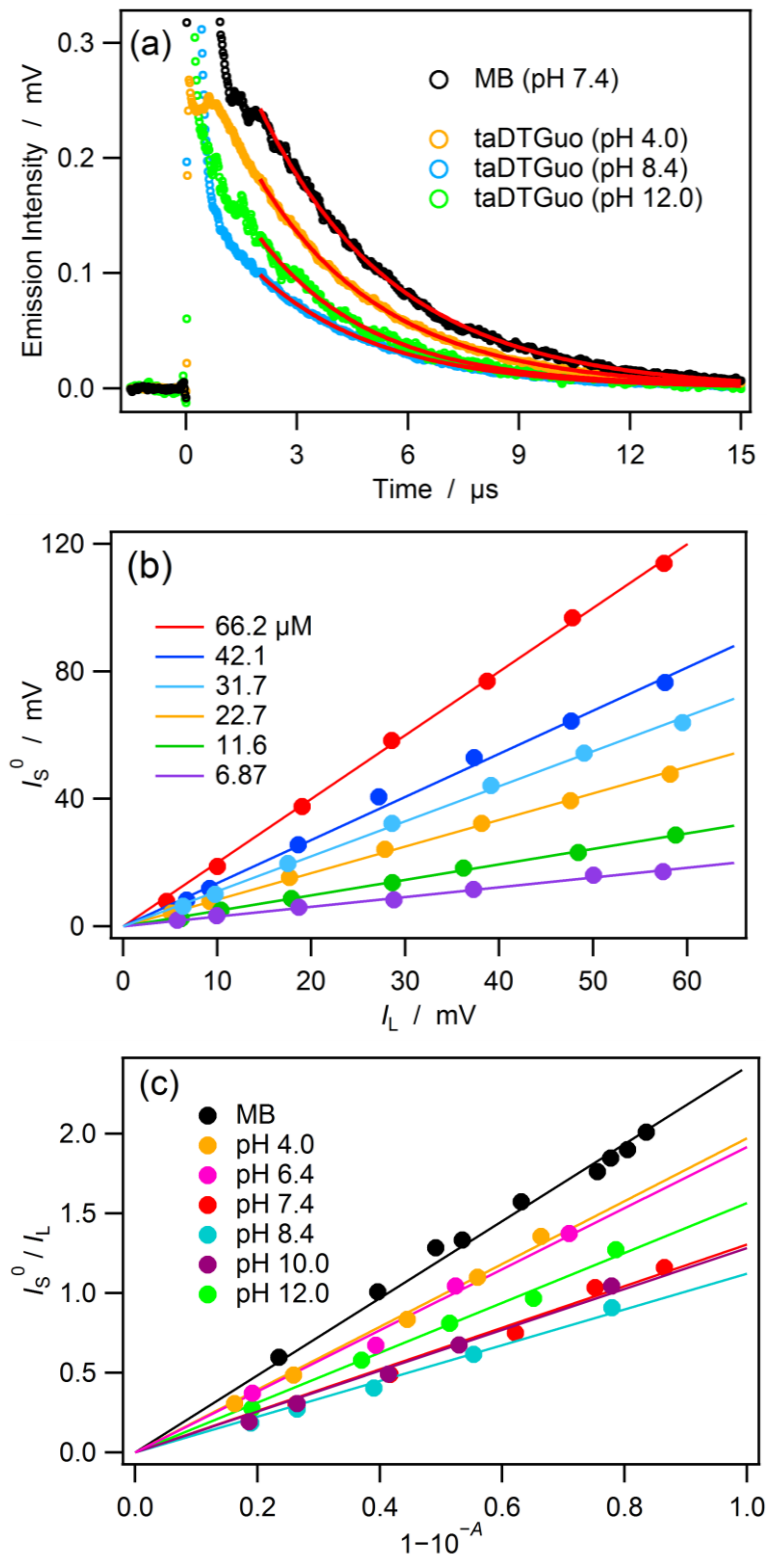**Figure 3.** S. Miyata *et al*.
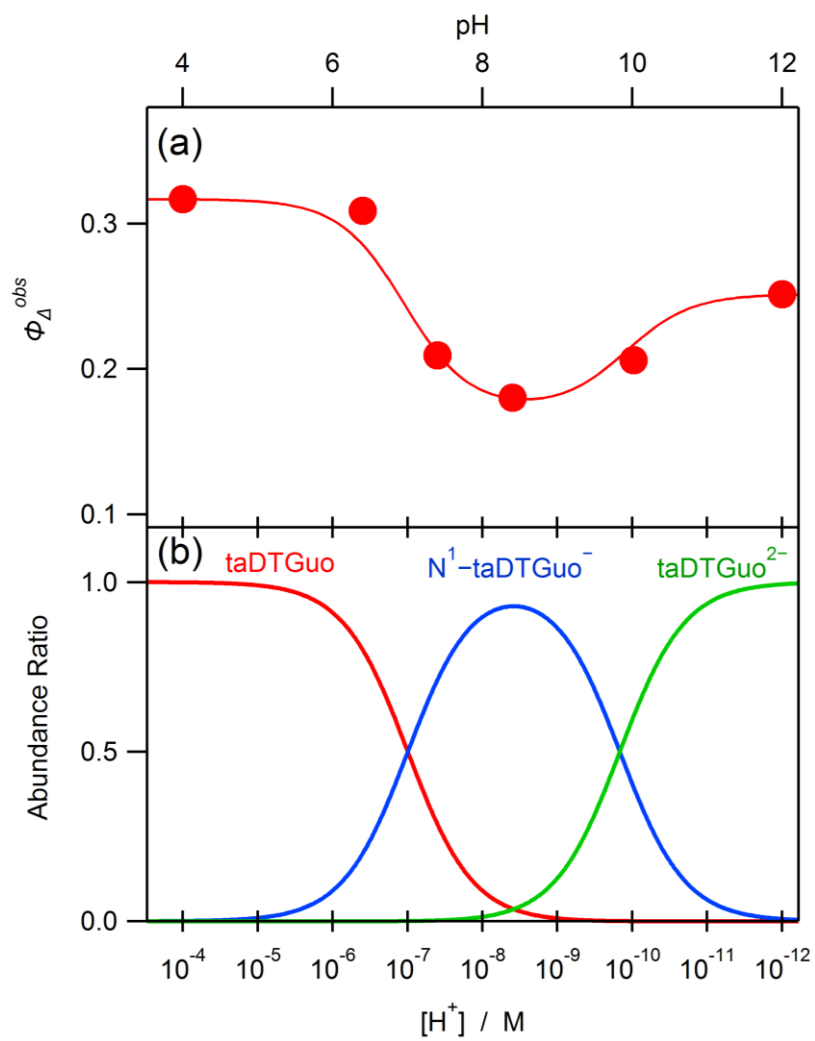
Figure 4.   S. Miyata *et al*.

Figure 5. S. Miyata *et al.*

Figure 6. S. Miyata *et al*.

TOC IMAGE